

Fabrication and Characterization of Graphene Incorporated Cu Based Perovskite in Application of Perovskite Solar Cell under Ambient Condition

Shah Sultan Ashrafi*, Kamal Hossain, Farid Ahmed, Abul Hossain, Obaidur Rahman

Department of Physics, Jahangirnagar University, Dhaka, Bangladesh

Email: *sultanaashrafi63@gmail.com

How to cite this paper: Ashrafi, S.S., Hossain, K., Ahmed, F., Hossain, A. and Rahman, O. (2020) Fabrication and Characterization of Graphene Incorporated Cu Based Perovskite in Application of Perovskite Solar Cell under Ambient Condition. *Advances in Materials Physics and Chemistry*, **10**, 1-16.
<https://doi.org/10.4236/ampc.2020.101001>

Received: January 27, 2019

Accepted: January 11, 2020

Published: January 14, 2020

Copyright © 2020 by author(s) and Scientific Research Publishing Inc. This work is licensed under the Creative Commons Attribution International License (CC BY 4.0).
<http://creativecommons.org/licenses/by/4.0/>



Open Access

Abstract

In this work, we demonstrate the synthesis and characterization of Cu-based thin film perovskites and their prospective application in photovoltaic cells and light-harvesting devices, which is lead(Pb) free and environmental friendly. We studied valuable part of graphene for stability issue in $\text{CH}_3\text{NH}_3\text{CuCl}_3$ (MACuCl_3) Perovskites solar cell and improved band gap 2.61 eV to 2.56 eV as well. Copper ions represented responsible of this materials for the bright green photoluminescence. For assimilating MACuCl_3 and G- MACuCl_3 based Perovskites, solar cells architectures and photovoltaic performance are argued among them. The main limitations for the solar cell efficiency were found the arrangement of insubstantial mass and high absorption coefficient of the electrons as well. As per as our knowledge, this work is demonstrated of the prospective of thin film MACuCl_3 and G- MACuCl_3 perovskite as light absorber and puts down the establishment for additional development of perovskite solar cell as alternative of lead-free materials.

Keywords

Demonstration, Perovskites, Light-Harvesting, MACuCl_3 , Absorber, Photoluminescence

1. Introduction

Recent improvement of Perovskites solar cells in efficiency is getting more and more attention based on lead halide perovskites. Beside Pb metal, many other metals like Sn, Cu, Be and so on are used to the compositional change for fabricating perovskites solar cells device. Within very short time last 10 years, the

wonderful power conversion efficiency (PCE%) was achieved rapidly from 3.8% to 22.1% in 2009 to 2019 [1] [2] [3]. Though organic-inorganic lead halide or mixed halide perovskites show excellent performance in photovoltaic cell device addressing 22.1% power conversion efficiency (PCE%), these perovskites experience from contamination, full content of poisonous and toxic which obstruct their commercialization [4]. To create large uniform crystallite size for perovskites materials for improving stabilization of perovskite device performance and develop the materials properties graphene composition are used in earlier reports. Grain size eventually led to roughness and high efficiency of photovoltaic cells [5] [6] [7]. Organic-inorganic lead halide perovskites have elated breach PCE% of solar cell in last six years [8]. In sequence with methylammonium lead iodide ($\text{CH}_3\text{NH}_3\text{PbI}_3$), they have been demonstrated for their excellent performance of high absorption coefficient, diffusion length and low defect density [9] [10] [11] [12] [13]. NREL's report establishing perovskites power conversion efficiency 22.1% has been achieved which is effective for replacing commercially successful polycrystalline silicon based solar cells and challenging to deposit thin film perovskites solar cells [14] [15] [16]. Suitable molecular proposal will be required to progress the material's assets and solar cell performance satisfying the gap $\text{CH}_3\text{NH}_3\text{CuCl}_3$ based perovskite. In the ecosystem due to its bioaccumulation and toxicity, Lead content of these materials has elevated concerns which obstruct the perovskites' pathway to commercialization. So it is very important to study and construct alternative modules of lead-free perovskites for optoelectronic and commercialization applications [17] [18] [19], thanks to prosperous chemistry for their expand synthetic path of new perovskites working field for photovoltaic and light harvesting applications looking up the tenability of the material [20]. The general formula may be written as $(\text{CH}_3\text{NH}_3)_2\text{A}_{(n-1)}\text{MnX}_{(3n+1)}$, where n is the number of layers within an inorganic block [21]. The thin film structure can be resultant by cutting the standard three dimensional perovskite along specific orientations ((110), (111) and (100)) and support to alternating organic and inorganic slabs [22]. At high temperature superconductor $\text{La}_{2-x}\text{Ba}_x\text{CuO}_4$ and the Ruddlesden Popper phase like K_2NiF_4 are iso-structural compounds because of their smaller ionic radii of transition metals [23]. Copper ion is predominantly motivating due to the ability to form compounds with large absorption coefficient in the visible region and the steadiness of this oxidation state in the environment [24]. Even with larger organo-ammonium cations and contributing wider synthetic tenability, the Jahn-Teller distortion begins flexible semi-coordinate bonds in the inorganic planes, which present higher plasticity and gracefulness to the structure, consequential in an easier interaction [25] [26]. Copper based thin film perovskites have been previously studied mainly for their interesting optical and magnetic properties where they perform like quasi-two dimension Heisenberg ferromagnetisms [27]. Currently [EDBE] (CuCl_4), where EDBE = 2,2'-(ethylenedioxy) bis (ethylammonium), has been realized Lithium ions(Li^+) batteries as cathode material [28]. Through the em-

ploy of an air blowing method toting up CuX (X = F, Cl, Br and I) to the perovskite pioneers optoelectronic properties of perovskite solar cells were enhanced in previous reports [29] [30]. To obtain the more stability of these materials against moisture Lead based arrangement with lower dimensionality and the 2D system with perovskite associated structure $\text{CH}_3\text{CH}_2\text{NH}_3\text{PbI}_3$ was exposed to perform as sensitizer in solar cells [31]. Even at 5% addition of Cu at the Pb position, the perovskite crystals preserved their cubic symmetry and photovoltaic cells with supplementary CuBr attributed larger perovskite grain sizes and enhanced power conversion efficiencies (PCE%) [32]. Due to the enlarge in tortuosity of the pathway of the molecule circulating through the coating, composites including of layered clays or silicates isolated in a polymeric matrix have been comprehensively studied as barrier materials for oxygen and water. The $\text{CH}_3\text{NH}_3\text{CuCl}_3$ should not only be impervious to oxygen but also to moisture as well a crucial protective coating summarizing [33]. To improve as protective coating layers oxygen and moisture opposed to materials that are also extremely conductive can be realistically designed. It is indispensable to encompass higher thickness to boost the tortuosity in the path of water and gas molecules when a polymeric composite is utilized as a protective coating [34] [35]. The special effects of slight incorporation of transition metals [*e.g.* Cr^{2+} , Co^{2+} , Cu^{2+} , and Y^{3+}] into the FAP- bI_3 (HN=CHNH₃PbI₃) perovskite compounds on the optical absorption spectra, electronic structure and chemical shift have been scrutinized through first principle calculation [36]. Hence, the most important thing to select elements that have far above the ground hole and electron conductivity besides having good quality fence properties to water and gases, so that the thickness of the coating does not slow down charge transfer and hold back solar cells performance [37]. Imperfection free layer graphene has been demonstrated to be unreceptive to many gases and moisture and due to small inter layer spacing [38]. However, modest knowledge about magnetic, electric properties and optoelectronic properties of Cu-based hybrid halide or mixed halide perovskites and very few manifestation of photovoltaic action has been reported in this material set. Here we have studied magnetic, electric properties and optoelectronic properties of Cu based perovskites and demonstrated perovskites solar cells for Pb replacement in low down dimensionality systems. We report the synthesis and characterization of Cu based perovskite family with the general formula MACuCl_3 and G- MACuCl_3 with the endeavor of investigating the thin film deposition for commercial applications and studying the photovoltaic properties to discover their potential as light sensitizer in perovskites solar cells and their optoelectronic properties. The existence of Cl^- is indispensable to recover the material stability against copper oxidization and augment the perovskite crystallization. By mixing Graphene, the optical absorption can be refrained within the visible to near infrared ($\lambda = 300 - 900 \text{ nm}$) range. Based on the density functional theory (DFT) optical shift and transport properties of new compounds were dispersed and understood using calculations. In arrangement of Cu^+ trap state

was established to be accountable for an well-organized green emission of these perovskites. Different parameters of deposition and fabrication of thin film were discussed to optimize integration of these materials into a perovskites solar cells device structure. The solar cell performance and currently limiting factors of the power conversion efficiency of this device are discussed to afford guidelines for further investigation and optimization of lead-free perovskites.

2. Experimental Section

2.1. Synthesis of MACuCl₃ and G-MACuCl₃

Methylammonium chloride was synthesized by counteracting 30 mL methylamine (40% mono, from Qualikems) and 20 mL hydrochloric acid (32% in water, from Merck). The three arms flask was filled with methylamine and HCl is added drop wise with methylamine solution at (8°C - 10°C) for 1 h with stirring. As synthesized methylammonium chloride was kept in ice for bath 3 hours. The precipitation was removed by putting the solution on a dry oven and carefully eliminating the solvent at 60°C. The crystalline CH₃NH₃Cl was cleaned several times by diethyl ether (from Merck) and dried for 24 hours using dry oven at 60°C. Then dried light yellow white powder of CH₃NH₃Cl was collected. Precursor 0.168 g of CH₃NH₃Cl was dissolved into 5 mL N, N-dimethylformamide and 0.564 g CuCl₂ was dissolved into 5 mL N, N-dimethylformamide (1:1) separately. Then light yellow solution of CH₃NH₃CuCl₃ perovskites was obtained. Graphene was prepared according to a modified Hummer's Method and it was added at concentrations 0.05 g·ml⁻¹ at 45 mass% with pristine perovskite (**Figure 2(b)** and **Figure 2(c)**) solution to obtain G-MACuCl₃.

2.2. Device Fabrication

At low temperature TiO₂ solution was prepared using PEG (Polyethylene Glycol), Distilled water and TiO₂ respectively 1:20:3 ratio. PEG normally was used for better dispersion of solution to obtain uniform film [34]. The TiO₂ solution (3 mg/ml) was deposited on pre-cleaned ITO (ITO were cleaned by sequential 15 min sonication in warm distilled water, acetone and ethanol, pursued by drying in an oven at 60°C) substrates by Dr. Blade method. Then it was positioned on a hot plate set to 40°C for 10 min and at 70°C for 10 min and we transferred to furnace for annealing at 350°C for 20 min to improve the film stickiness. Then Perovskites (Pristine solution MACuCl₃, G-MACuCl₃) solution were deposited on TiO₂ film coated ITO using spin-coating method at 2000 rpm for 30 s [33] followed by heating at 80°C for 15 min until crystal growth. Graphite layer was coated by candle on the another ITO as the hole transport materials (HTM). Then both ITO were sandwiched together using two binder clips (**Figure 1(c)**).

2.3. Instruments and Characterizations

X-ray diffraction (XRD) data were composed on GBC EMMA X-ray diffractometer

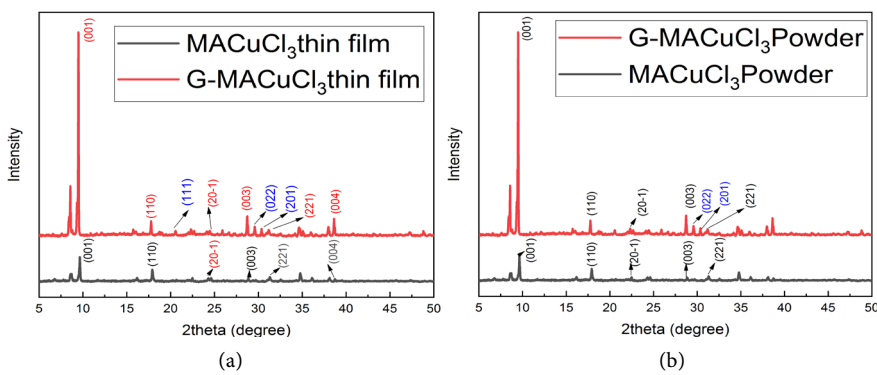


Figure 1. Comparison of X-ray diffraction of Methylammonium chloride, Methylammonium copper chloride (MACuCl_3) and graphene incorporated Methylammonium copper chloride (G-MACuCl_3) (a) for thin film and (b) for powder crystal respectively.

at Wazed Miah Science Research Center, Jahangirnagar University with Cu K α radiation ($\lambda = 1.54 \text{ \AA}$). The scanning angular range was $5^\circ \leq 2\theta \leq 50^\circ$ to get possible fundamental picks for each sample. UV-Vis spectrum of methylamine chloride, methylammonium copper chloride perovskite solution and methylammonium copper chloride graphene at 60°C was studied using the UV-Vis Spectrophotometer Model: UVS-2800 at wavelength range of 190 nm - 1100 nm and very low stray light and noise specifications. The IR spectra of the samples were verified at room temperature using a SHIMADZU, IR Tracer-100, Japan. The wave number range was from 400 cm^{-1} to 4000 cm^{-1} . The device performance was characterized without any encapsulation using solar simulator (IEC 60904-9 Edition2 and ASTM E927-10 standards, BCSIR, Bangladesh) under an AM1.5G filter at 100 mW/cm^2 in air and the intensity was standardized using a certified perovskite photodiode.

3. Results and Discussion

3.1. Characterization of Perovskites Properties from X-Ray Diffraction Measurement

Before **Figure 1(a)** shows the XRD peaks of synthesized thin film Methylammonium copper chloride and graphene incorporated methylammonium copper chloride. Diffraction peaks at 9.38° , 17.67° , and 28.81° are indexed to be (001), (110), and (003) for $\text{CH}_3\text{NH}_3\text{CuCl}_3$ crystal planes, and other peaks are assigned to the glass substrate. For graphene assisted perovskite we observed new planes (111), (022) and (201) attributed at 20.53° , 29.54° and 30.36° respectively in the XRD. In further we can progress crystallinity with the incorporation of graphene which was exposed by the intensity change in the (001) plane. We analyzed the crystallite size full and width half maxima (FWHM) for MCl , MACuCl_3 and G-MACuCl_3 viewed that the FWHM is smallest for G-MACuCl_3 demonstrating the highest crystallinity of the perovskite phase in the (001) plane attributed 9.38° . However, the peak widths at half-maxima are about the same for both samples after normalizing the perovskite (001) peak intensities, denotation that

on average, the differences in crystallinity are not significant. The average crystallites size were measured 43.015 nm for MACuCl_3 and 63.135 nm for Graphene- MACuCl_3 powder crystal (**Figure 1(b)**) which assembled uniformly due to sharp peaks achieved. The first order peak maxima synthesized thin film (001) for Methylammonium copper chloride and crystallite size also increased 180.44 nm and 200.56 nm respectively compare to the powder XRD reading and all are monoclinic lattice system. Volume of unit cell MACuCl_3 and graphene incorporated MACuCl_3 perovskite is $783(\text{\AA})^3$ and $1200.2(\text{\AA})^3$ respectively (**Table 1**). Thin film X-ray diffraction patterns of these two films are revealed in **Figure 1(a)** and compared to their respective powders. In both the cases, the (00l) reflections are finer [37], the annealing conditions were optimized to acquire crystalline, single-phase films.

3.2. Investigation of Structural Properties of Perovskites by Fourier Transformation Infrared (FTIR) Measurement

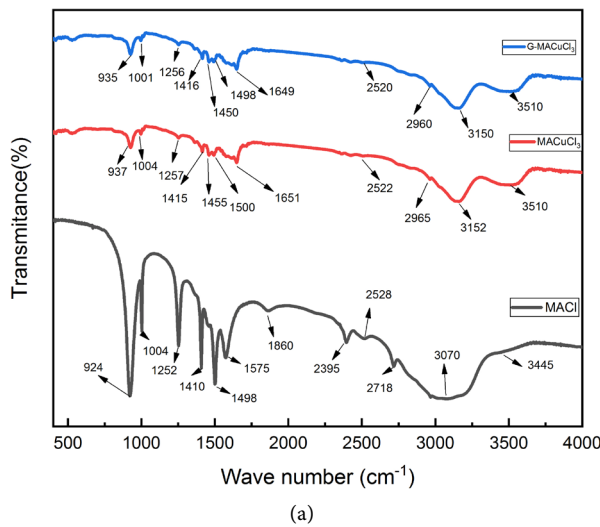
There are several peaks of these three FTIR curves in the FTIR spectrum of MACuCl_3 and G- MACuCl_3 (**Figure 2(b)**) have a broad band at about 3510 cm^{-1} which indicate the water bond O-H stretching which are not present in MACl . The second vibration mode 3052 cm^{-1} of MACuCl_3 and 3050 cm^{-1} for G- MACuCl_3 which indicates the alkanes groups of C-H stretching but this curve is smaller than MACl . The spectrum (black) represents the large cation salt methylammonium chloride. In this curve the bond C-H is stretching alkanes, C-N stretching amines, alkanes bending C-H and bending C-O are present [33] Similar vibration mode 1651 cm^{-1} is attributed at both materials as synthesized MACuCl_3 and G- MACuCl_3 , which is not found in MAI. The vibrational mode 1651 cm^{-1} indicates the carbon-oxygen stretching [34].

3.3. Characterization of Optoelectronic Properties of Materials

On site Coulomb interactions with the DFT method together (U+DFT) was used to schoolwork the electronic structure of copper perovskite materials. These copper ions(Cu^+) enclosing compounds illustrate the most unwavering ferromagnetic configuration within self-governing inorganic planes, while the interplanar

Table 1. Crystal structure and lattice parameters of cu-based perovskites (using XRD data by full proof software).

Formula	Crystal System	a [Å]	b [Å]	c [Å]	β [deg]	Volume of unit cell (Å) ³
Thin film MACuCl_3	monoclinic	19.86	3.61	11.01	97	783
Thin film G- MACuCl_3	monoclinic	20.03	3.09	19.39	90.74	1200
Powder MACuCl_3	monoclinic	18.8	4.23	11.11	98	875
Powder G- MACuCl_3	monoclinic	20.02	4.31	17.51	92	1508



(a)



(b)

(c)

Figure 2. (a) Comparison Fourier transform infrared (FTIR) of Methylammonium chloride (MACl), Methylammonium copper chloride (MACuCl₃) and Methylammonium copper chloride graphene composite (G-MACuCl₃), (b) Perovskite crystal of MACuCl₃ and (c) Perovskite crystal of graphene-MACuCl₃.

Table 2. Fourier Transformation Infrared (FTIR) Characterization of Materials.

Vibration (cm ⁻¹) mode of MACuCl ₃	Vibration (cm ⁻¹) mode of G-MACuCl ₃	Attributed
3510	3510	O-H Stretch
3152	33,150	N-H Stretch
2965	2960	C-H Stretch
2522	2520	unidentified
1651	1649	C-O [34]
1500	1498	NH ₃ bending
1455	1450	NH ₃ bending
1415	1416	CH ₃ bending
1257	1256	CH ₃ -NH ₃ rocking
1004	1001	unidentified
937	935	CH ₃ -NH ₃ rocking

pairing is anti-ferromagnetic (AFM), corresponding with previous electronic and magnetic studies of $(\text{CH}_3\text{NH}_3)_2\text{CuCl}_4$ [38]. The absorption spectra of the series MACuCl_3 and G-MACuCl_3 show typical features improving absorbance [35] of graphene incorporated and highest absorption peak 341 nm and 243.25 nm respectively (**Figure 3(a)**). Strong bands for each material with coefficient absorption up to 200 cm^{-1} are originated below 350 nm, and determined the corresponding band gaps from Tauc plots (**Figure 3(c)** and **Figure 3(d)**) are 2.60 eV (477 nm) for powder MACuCl_3 , 2.61 eV (475 nm) for powder G-MACuCl_3 , 2.61 eV (474 nm) for thin film MACuCl_3 and improved band gap 2.56 eV (483 nm) for thin film G-MACuCl_3 (**Table 3**). MACuCl_3 and G-MACuCl_3 were referred for future optimization by good feature of their better stability and improved optoelectronic properties, respectively [36]. ITO films acquired a high excellence transparent electrode which has been measured low resistance as per $10 \Omega\text{-cm}$ and an elevated optical transmittance in the visible range by RF sputtering and premeditated their application as transparent electrodes in outsized area electric devices [39].

Multilayer films with high absorbance and visible transmittance below 20% were demonstrated as like ITO/TiO₂, ITO/TiO₂/MACuCl₃ and ITO/TiO₂G-MACuCl₃ by sputtering at room temperature and examined the electrical and optical

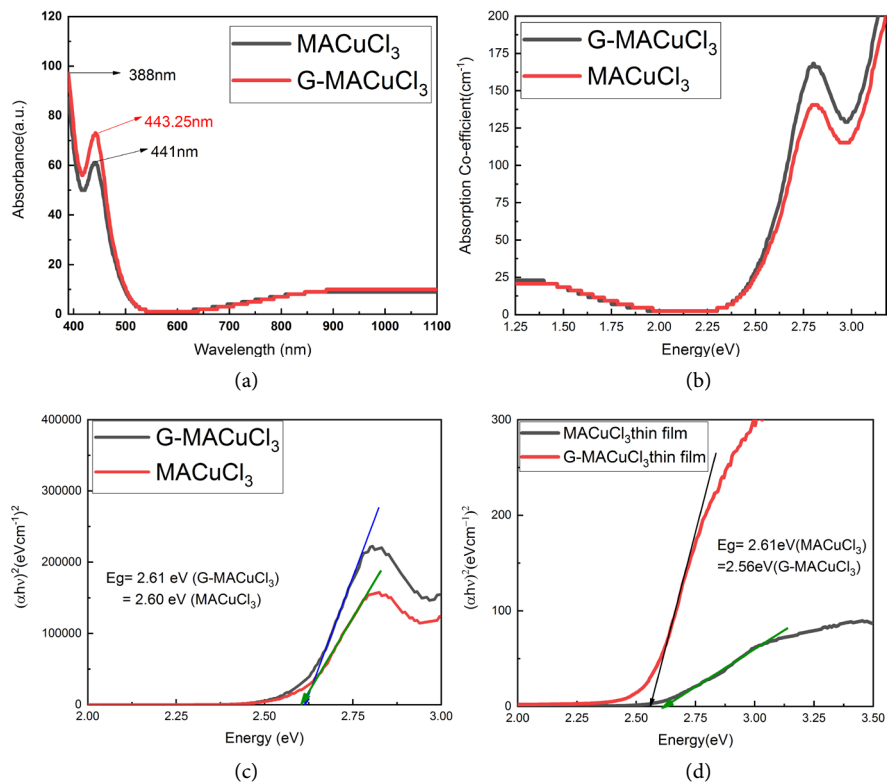


Figure 3. (a) Comparison uv-visible spectra of Methylammonium copper chloride (MACuCl_3) and Methylammonium copper chloride graphene composite (G-MACuCl_3), (b) Comparison coefficient of absorbance spectra of MACuCl_3 and G-MACuCl_3 , (c) Tauc plot of MACuCl_3 and G-MACuCl_3 for band gap calculation for powder and (d) for thin film.

Table 3. Band gap of perovskites.

Cu based perovskites	Band gap (eV)
Powder MACuCl ₃	2.60
Powder G-MACuCl ₃	2.61
Thin film MACuCl ₃	2.61
Thin film G-MACuCl ₃	2.56

characteristics of multilayer structures and single-layer (**Figure 4(a)** and **Figure 4(b)**). Besides, the transmittance is found to be mainly reliant on the thickness of TiO₂ film. Based on **Figure 4(b)** it can be observed that multilayer ITO/TiO₂/MACuCl₃ and ITO/TiO₂G-MACuCl₃ films show higher absorbance than pure ITO film.

3.4. Current Density-Voltage Investigation

Current density-Voltage (J-V) curves were found after enlightening the CH₃NH₃CuCl₃ and Graphene-CH₃NH₃CuCl₃ solar cells under ambient condition. The undefended CH₃NH₃CuCl₃ cells illustrated a rapid decline in the short-circuit current and open circuit-voltage (**Figure 5(c)** and **Figure 5(d)**). After 40 days of revelation to moisture, photovoltaic behavior is investigated from the cells. **Figure 5(a)** and **Figure 5(b)** shows the J-V curves of CH₃NH₃CuCl₃ solar cells summarized with graphene composite. For graphene composition enhanced the stability of the cells to moisture. This explains why graphene composite demonstrate good stability in towering humidity conditions. The best performing cell with a self-protective coating confirmed a photocurrent of 0.21 mA·cm⁻² and an open-circuit voltage of 334 mV. The low open-circuit voltage found when compared to the best performing cell in literature deposited with graphite is due to the high recombination losses with CH₃NH₃CuCl₃ [39]. Changing graphene concentration that exhibits lower recombination sufferers than CH₃NH₃CuCl₃ and the performance of the photovoltaic device can be further optimized. Devices were fabricated with ITO/TiO₂/CH₃NH₃CuCl₃/graphite/ITO consuming graphite itself as the HTM established higher open-circuit voltage of 0.334 V, but lower short-circuit current density of 0.039 mA·cm⁻² (**Table 4**) due to low conductivity of graphene compared with CH₃NH₃CuCl₃ (**Figure 5(c)** and **Figure 5(d)**). Utilizing of more conductive materials further optimization, graphene can also progress the stability of the devices. Photocurrent vibrations is pragmatic in samples with copper based perovskites and with composition of graphene this could be due to the graphene incorporation performing as a buffer layer and avoiding the direct contact of TiO₂ and the graphite HTM [40]. The crystal size during the CH₃NH₃CuCl₃ growth is also another factor that can set in to the variation of photocurrents and therefore claims photocurrents decreasing with regards to the graphene incorporation. The shunt (R_{SH}) and series resistances (R_S) are considered to study the effect of graphene self-protective coating on the electrical

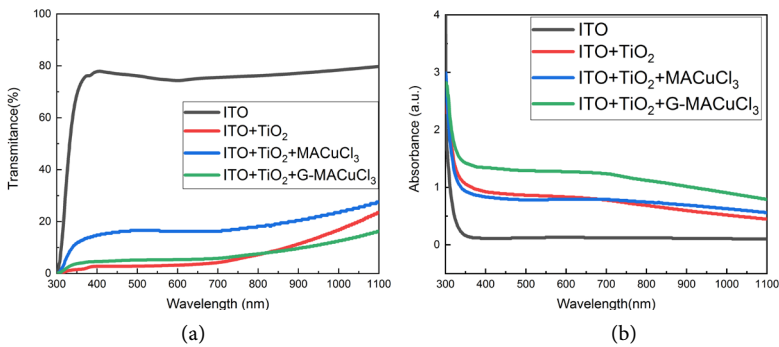


Figure 4. (a) Comparison transmittance spectra of ITO, Titanium dioxide (TiO_2), Methylammonium copper chloride (MACuCl_3) and graphene incorporated Methylammonium copper chloride (G- MACuCl_3) layers. (b) Comparison absorbance spectra of ITO, Titanium dioxide (TiO_2), Methylammonium copper chloride (MACuCl_3) and graphene incorporated Methylammonium copper chloride (G- MACuCl_3) layers.

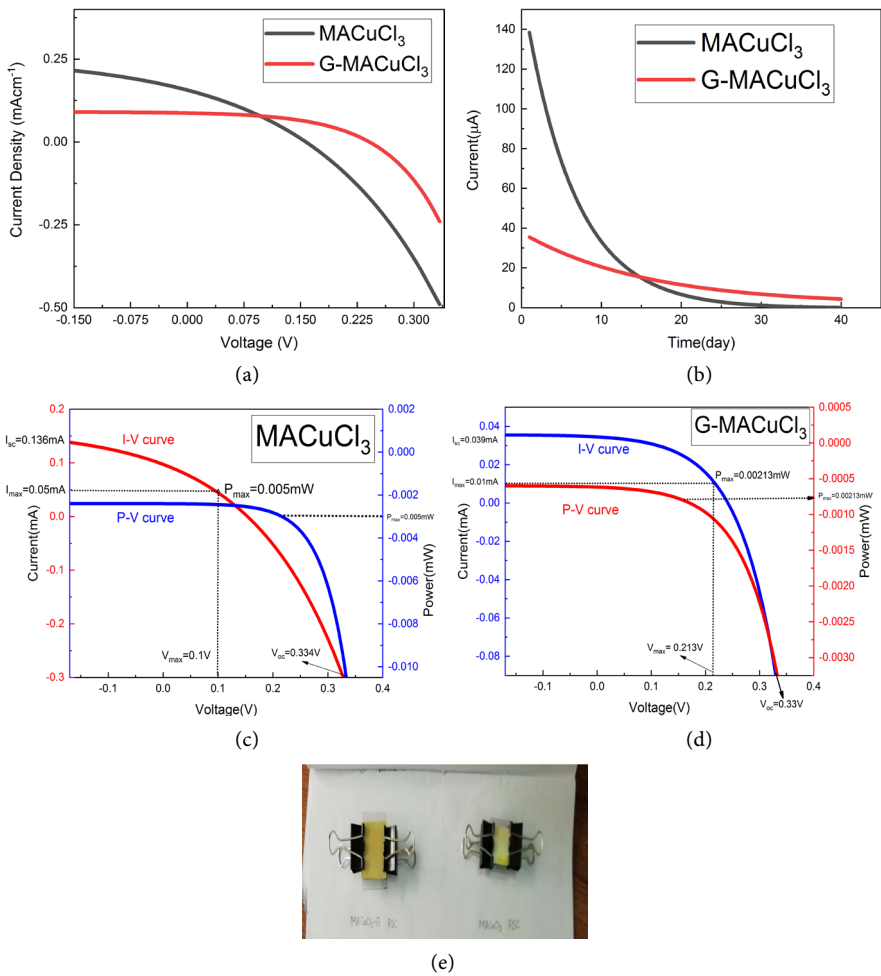


Figure 5. (a) Comparison Current density ($\text{J}_{sc} \text{ mA cm}^{-2}$)-Voltage of MACuCl_3 based solar cell and graphene incorporated G- MACuCl_3 , (b) Ageing effect on solar cell performance, (c) Current(mA)-Voltage(V) and Power(mW)-Voltage(V) curve of Methylammonium copper chloride (MACuCl_3) and (d) Current(mA)-Voltage(V) and Power(mW)-Voltage(V) curve of graphene incorporated Methylammonium copper chloride (G- MACuCl_3), (e) Solar cells of following materials.

Table 4. Performance of photovoltaic cells.

Solar Cells	Current density (mA·cm ⁻²)	Fill Factor (FF%)	Open Circuit-Voltage (mV)	Short Circuit-Current (mA)	Power Conversion Efficiency (PCE%)
MACuCl ₃	0.21	42.82	334	0.136	1.52×10^{-3}
G-MACuCl ₃	0.11	47.45	330	0.039	6.45×10^{-4}

performance of the devices using the J-V data of the devices in **Figure 5**. The degradation of the perovskite due to the diffusion of oxygen and moisture into the perovskite layer was investigated. In spite of the shunt and series resistances of the cells, we look forward to the perovskite degradation machinery to be the identical. Therefore, the results of the achieved with higher series resistances and lower shunt (compared to best performing cells) could be unmitigated to high efficiency cells [40]. We finished a reference cell without protective coating and compared our power conversion efficiency to make sure suitable comparison.

The device without any graphene revealed a 15.5 KΩ of R_{SH} and a 2.4 KΩ of R_S. Where the device one with graphene composite illustrated a increase in both R_{SH} and R_S to a 61 KΩ and 29 KΩ respectively. Although the R_{SH} and R_S resistances are increasing with increase of graphene composition, but the ratio of R_{SH}/R_S has reduced from 6.45 to 2.11 for the devices without graphene and with graphene. Due to graphene incorporated into the perovskite a larger nanocomposite is fashioned which volume of unit cell increased 783 (Å)³ to 1200 (Å)³ (see **Table 1**) results in a augment in the R_S of the coated devices. Beside that holes of CuCl and the conduction band electrons of TiO₂ show the way to the lower shunt resistance(R_{SH}) due to CuCl may come in contact with the TiO₂ [41]. Low conductivity of without graphene compared to the graphene composite of perovskites because of reduce in the R_{SH} [42]. **Figure 5(c)** and **Figure 5(d)** showed using graphite as HTM and 8 μm TiO₂, solar cell devices were realized with MACuCl₃ and Graphene-MACuCl₃ characterized. MACuCl₃ consented a power conversion efficiency of 0.00152%, with V_{oc} = 334 mV, J_{sc} = 215 μA/cm², and FF = 42.82%. Graphene-MACuCl₃ gave a much lower power conversion efficiency of 0.00065%, though the optimized band gap (2.56 eV) less than MACuCl₃ and J_{sc} = 112 μA/cm², V_{oc} = 330 mV, and FF = 0.47 (**Table 4**). Because of Cu²⁺ reduction (as confirmed by XPS and photoluminescence measurements) the higher trap density commenced for lower performance of Graphene-MACuCl₃ which establish an additional way for charge recombination. To bear out the repairing behavior of the cell operating under dark condition (**Figure 5(a)**) the two devices was investigated in a wider range from -5V to +5V for dark current. High dark currents found (**Figures 5(a)-(c)**) at existence of high leakage current probably due to the direct make contact between the TiO₂ and graphite (HTM), assisted by the absence of perovskite checking layer over the TiO₂. Another limitation factor, band gap 2.61 eV and 2.56 eV suggesting deprived electron transfer in the device (**Figure 3(d)**) from ultraviolet photoelectron spectroscopy (UVS-2800) mea-

surements. The devices based on MACuCl_3 and G- MACuCl_3 were demonstrated the sensitization action of the perovskite (see **Figure 5(e)**) in photocurrent measurements. The measurement was presented using Solar simulator (1.5 AM at 25°C and power 1KW, BCSIR, Dhaka, Bangladesh). In précis, graphene composite has been found to perform as a multifunctional coating facilitating charge-carrier transport while simultaneously as long as an impervious seal to moisture [43], representing a corroboration of perception composite coating for superior photovoltaic stability [44]. The composite averts degradation of the $\text{CH}_3\text{NH}_3\text{CuCl}_3$ from UV, moisture, and air as revealed by the constant short circuit current density over an absolute period of time. The shielding graphene composite successfully checks the corrosion of the $\text{CH}_3\text{NH}_3\text{CuCl}_3$ into the Cl_2 and CuCl_2 [45]. The processing of $\text{CH}_3\text{NH}_3\text{CuCl}_3$ cells under atmospheric conditions once they are summarized with graphene composite which could allow the high moisture impermeability. In this work for both oxygen and moisture sensitive use of composite defensive materials could be comprehensive other lead free organic-inorganic metal halide perovskites. In this paper the sandwich approach could build up opportunities for coated or roll to roll perovskite cells and suggest important diminution in the processing costs. The use of coated counter electrode and the optimization of the composite for the cells continuing efforts engage fabrication of higher efficiency cells with graphite. It is currently followed using graphene with $\text{CH}_3\text{NH}_3\text{CuCl}_3$ crystals to prevent moisture from solar cells atmospheric roll to roll process is used. Similar perception can also be useful to design and widen different materials for lamination to grant long term stability.

4. Conclusion

Photo-voltaic properties and material stability of thin film perovskites $\text{CH}_3\text{NH}_3\text{CuCl}_3$ and with graphene composite are investigated in details, where it is found to be strongly dependent on the graphene composite. The absorption is occupied by their connected band gap that can be refrained diminishing from 2.61 eV to 2.56 eV in graphene composite. An additional donation to the absorption in the region between 350 and 900 nm is experimented from graphene transitions. Based on Cu perovskite and with graphene composite, they are fabricated with uniform penetration of mesoporous TiO_2 using thin film copper perovskites which realized PCE(%) of 0.00152% sing MACuCl_3 as sensitizer. Moreover, these graphene incorporated perovskites solar cells have been achieved highest fill factor 47.45% which affected solar cell performance. In spite of the mesoporous TiO_2 layer having been revealed to help the electron withdrawal from the thin film perovskites, low absorption coefficient and lower volume of unit cell for the electron cooperation of solar cell efficiency is good. This demonstration introduced to improve of photo-voltaic cell and overcome these issues stressing the importance of investigation.

Acknowledgements

OR thanks to UGC base research fellowship. The authors acknowledge Shahriar

Bashar, Senior Scientific Officer, BCSIR, Dhaka and Khairul Islam, Scientific Officer, WMSRC, Jahangirnagar University for performing PCE% measurements on the perovskite samples and the CMP Lab, JU for Renewable Energy Research for experimental facilities.

Conflicts of Interest

The authors declare no conflicts of interest regarding the publication of this paper.

Authors Contributions

KH, SA and OR developed the idea of using graphite as a HTM. SA and KH donated equally to this work. SA and KH formulated the experimental plan and completed the experiments. All the authors analyzed and talked about the data and co-wrote the manuscript. KH, SA and OR developed the idea of using graphite as a HTM. SA and KH donated equally to this work.

References

- [1] Miyasaka, T. (2015) Perovskite Photovoltaics: Rare Functions of Organo Lead Halide in Solar Cells and Optoelectronic Devices. *Chemistry Letters*, **44**, 720-729. <https://doi.org/10.1246/cl.150175>
- [2] Kojima, A., Teshima, K., Shirai, Y. and Miyasaka, T. (2009) Organometal Halide Perovskites as Visible-Light Sensitizers for Photovoltaic Cells. *Journal of the American Chemical Society*, **131**, 6050-6051. <https://doi.org/10.1021/ja809598r>
- [3] NREL Chart. http://www.nrel.gov/ncpv/images/efficiency_chart.jpg
- [4] Hao, F., Stoumpos, C.C., Cao, D.H., Chang, R.P.H. and Kanatzidis, M.G. (2014) Lead-Free Solid-State Organic-Inorganic Halide Perovskite Solar Cells. *Nature Photonics*, **8**, 489-494. <https://doi.org/10.1038/nphoton.2014.82>
- [5] Kamat, P.V. (2014) Organometal Halide Perovskites for Transformative Photovoltaics. *Journal of the American Chemical Society*, **136**, 3713-3714. <https://doi.org/10.1021/ja501108n>
- [6] Kim, H.-S., Im, S.H. and Park, N.-G. (2014) Organolead Halide Perovskite: New Horizons in Solar Cell Research. *The Journal of Physical Chemistry C*, **118**, 5615-5625. <https://doi.org/10.1021/jp409025w>
- [7] Park, J.-H., *et al.* (2011) Effects of Deposition Temperature on Characteristics of Ga-Doped ZnO Film Prepared by Highly Efficient Cylindrical Rotating Magnetron Sputtering for Organic Solar Cells. *Solar Energy Materials and Solar Cells*, **95**, 657-663.
- [8] Im, J.-H., Lee, C.-R., Lee, J.-W., Park, S.-W. and Park, N.-G. (2011) 6.5% Efficient Perovskite Quantum-Dot-Sensitized Solar Cell. *Nanoscale*, **3**, 4088-4093. <https://doi.org/10.1039/c1nr10867k>
- [9] Kim, H.-S., Lee, C.-R., Im, J.-H., Lee, K.-B., Moehl, T., Marchioro, A., Moon, S.-J., Humphry-Baker, R., Yum, J.-H., Moser, J.E., Gratzel, M. and Park, N.-G. (2012) Lead Iodide Perovskite Sensitized All-Solid-State Submicron Thin Film Mesoscopic Solar Cell with Efficiency Exceeding 9%. *Scientific Reports*, **2**, Article No. 591. <https://doi.org/10.1038/srep00591>
- [10] Liu, M., Johnston, M.B. and Snaith, H.J. (2013) Efficient Planar Heterojunction Pe-

rovskite Solar Cells by Vapour Deposition. *Nature*, **501**, 395-398.

<https://doi.org/10.1038/nature12509>

- [11] Hu, Q., Wu, J., Jiang, C., Liu, T., Que, X., Zhu, R. and Gong, Q. (2014) Engineering of Electron-Selective Contact for Perovskite Solar Cells with Efficiency Exceeding 15%. *ACS Nano*, **8**, 10161-10167. <https://doi.org/10.1021/nn5029828>
- [12] Nie, W., Tsai, H., Asadpour, R., Blancon, J.-C., Neukirch, A.J., Gupta, G., Crochet, J.J., Chhowalla, M., Tretiak, S., Alam, M.A., Wang, H.-L. and Mohite, A.D. (2015) High-Efficiency Solution-Processed Perovskite Solar Cells with Millimeter-Scale Grains. *Science*, **347**, 522-525. <https://doi.org/10.1126/science.aaa0472>
- [13] Burschka, J., Pellet, N., Moon, S.-J., Humphry Baker, R., Gao, P., Nazeeruddin, M. and Graetzel, M. (2013) Sequential Deposition as a Route to High-Performance Perovskite-Sensitized Solar Cells. *Nature*, **499**, 316-319. <https://doi.org/10.1038/nature12340>
- [14] Green, M.A., Emery, K., Hishikawa, Y., Warta, W. and Dunlop, E.D. (2014) Solar Cell Efficiency Tables (Version 44). *Progress in Photovoltaics*, **22**, 701-710. <https://doi.org/10.1002/pip.2525>
- [15] Snaith, H. (2013) Perovskites: The Emergence of a New Era for Low-Cost, High-Efficiency Solar Cells. *The Journal of Physical Chemistry Letters*, **4**, 3623-3630. <https://doi.org/10.1021/jz4020162>
- [16] Green, M.A., Ho-Baillie, A. and Snaith, H.J. (2014) The Emergence of Perovskite Solar Cells. *Nature Photonics*, **8**, 506-514. <https://doi.org/10.1038/nphoton.2014.134>
- [17] Stranks, S.D. and Snaith, H.J. (2015) Metal-Halide Perovskites for Photovoltaic and Light-Emitting Devices. *Nature Nanotechnology*, **10**, 391-402. <https://doi.org/10.1038/nnano.2015.90>
- [18] Zhang, W., Saliba, M., Moore, D.T., Pathak, S.K., Horantner, M.T., Stergiopoulos, T., Stranks, S.D., Eperon, G.E., AlexanderWebber, J.A., Abate, A., Sadhanala, A., Yao, S., Chen, Y., Friend, R.H., Estroff, L.A., Wiesner, U. and Snaith, H.J. (2015) Ultrasmooth Organic-Inorganic Perovskite Thin-Film Formation and Crystallization for Efficient Planar Heterojunction Solar Cells. *Nature Communications*, **6**, Article No. 6142. <https://doi.org/10.1038/ncomms7142>
- [19] Boix, P.P., Nonomura, K., Mathews, N. and Mhaisalkar, S.G. (2014) Current Progress and Future Perspectives for Organic/Inorganic Perovskite Solar Cells. *Materials Today*, **17**, 16-23. <https://doi.org/10.1016/j.mattod.2013.12.002>
- [20] Xing, G., Mathews, N., Lim, S., Yantara, N., Liu, X., Sabba, D., Graetzel, M., Mhaisalkar, S. and Sum, T. (2014) Low-Temperature Solution-Processed Wavelength-Tunable Perovskites for Lasing. *Nature Materials*, **13**, 476-480. <https://doi.org/10.1038/nmat3911>
- [21] Zhou, H., Chen, Q., Li, G., Luo, S., Song, T.-B., Duan, H.-S., Hong, Z., You, J., Liu, Y. and Yang, Y. (2014) Interface Engineering of Highly Efficient Perovskite Solar Cells. *Science*, **345**, 542-546. <https://doi.org/10.1126/science.1254050>
- [22] Gao, P., Gratzel, M. and Nazeeruddin, M.K. (2014) Organohalide Lead Perovskites for Photovoltaic Applications. *Energy & Environmental Science*, **7**, 2448-2463. <https://doi.org/10.1039/C4EE00942H>
- [23] Mitzi, D.B. (2005) Hybrid Organic-Inorganic Electronics. In: *Functional Hybrid Materials*, Wiley, Hoboken, 347-386. <https://doi.org/10.1002/3527602372.ch10>
- [24] Mitzi, D.B. and Brock, P. (2001) Structure and Optical Properties of Several Organic-Inorganic Hybrids Containing Corner-Sharing Chains of Bismuth Iodide Octahedra. *Inorganic Chemistry*, **40**, 2096-2104.
- [25] Mitzi, D.B. (2007) Synthesis, Structure, and Properties of Organic Inorganic Pe-

- rovskites and Related Materials. In: *Progress in Inorganic Chemistry*, John Wiley & Sons, Inc., Hoboken, 1-121. <https://doi.org/10.1002/9780470166499.ch1>
- [26] Greenwood, N.N. and Earnshaw, A. (1984) Chemistry of the Elements. Pergamon Press, Oxford.
- [27] Willett, R., Place, H. and Middleton, M. (1988) Crystal Structures of Three New Copper (II) Halide Layered Perovskites: Structural, Crystallographic, and Magnetic Correlations. *Journal of the American Chemical Society*, **110**, 8639-8650. <https://doi.org/10.1021/ja00234a010>
- [28] Snively, L.O., Drumheller, J.E. and Emerson, K. (1981) Magnetic Susceptibility of 1,4-Butanediammonium Tetrachlorocuprate. *Physical Review B: Condensed Matter and Materials Physics*, **23**, 6013-6017. <https://doi.org/10.1103/PhysRevB.23.6013>
- [29] Suzuki, A. and Oku, T. (2018) Effects of Transition Metals Incorporated into Perovskite Crystals on the Electronic Structures and Magnetic Properties by First-Principles Calculation. *Heliyon*, **4**, e00755. <https://doi.org/10.1016/j.heliyon.2018.e00755>
- [30] Suzuki, A. and Oku, T. (2019) First-Principles Calculation Study of Electronic Structures of Alkali Metals (Li, K, Na and Rb)-Incorporated Formamidinium Lead Halide Perovskite Compounds. *Applied Surface Science*, **483**, 912-921. <https://doi.org/10.1016/j.apsusc.2019.04.049>
- [31] Zhang, Y.-Y., Chen, S., Xu, P., Xiang, H., Gong, X.-G., Walsh, A. and Wei, S.-H. (2018) Intrinsic Instability of the Hybrid Halide Perovskite Semiconductor $\text{CH}_3\text{NH}_3\text{PbI}_3$. *Chinese Physics Letters*, **35**, Article ID: 036104. <https://doi.org/10.1088/0256-307X/35/3/036104>
- [32] Yin, W.-J., Yang, J.-H., Kang, J., Yan, Y. and Wei, S.-H. (2015) Halide Perovskite Materials for Solar Cells: A Theoretical Review. *Journal of Materials Chemistry A*, **3**, 8926-8942. <https://doi.org/10.1039/C4TA05033A>
- [33] Nalage, S.R., et al. (2012) Sol-Gel Synthesis of Nickel Oxide Thin Films and Their Characterization. *Thin Solid Films*, **520**, 4835-4840. <https://doi.org/10.1016/j.tsf.2012.02.072>
- [34] Park, Y.R. and Kim, K.J. (2003) Sol-Gel Preparation and Optical Characterization of NiO and $\text{Ni}_{1-x}\text{Zn}_x\text{O}$ Thin Films. *Journal of Crystal Growth*, **258**, 380-384. [https://doi.org/10.1016/S0022-0248\(03\)01560-4](https://doi.org/10.1016/S0022-0248(03)01560-4)
- [35] Cortecchia, D., et al. (2016) Lead-Free $\text{MA}_2\text{CuCl}_x\text{Br}_{4-x}$ Hybrid Perovskites. *Inorganic Chemistry*, **55**, 1044-1052.
- [36] Gomez, S., Urra, I., Valiente, R. and Rodriguez, F. (2010) Spectroscopic Study of Cu^{2+} and Cu^+ Ions in High-Transmission Glass. Electronic Structure and $\text{Cu}^{2+}/\text{Cu}^+$ Concentrations. *Journal of Physics: Condensed Matter*, **22**, Article ID: 295505. <https://doi.org/10.1088/0953-8984/22/29/295505>
- [37] Zolfaghari, P., de Wijs, G.A. and de Groot, R.A. (2013) The Electronic Structure of Organic-Inorganic Hybrid Compounds: $(\text{NH}_4)_2\text{CuCl}_4$, $(\text{CH}_3\text{NH}_3)_2\text{CuCl}_4$ and $(\text{C}_2\text{H}_5\text{NH}_3)_2\text{CuCl}_4$. *Journal of Physics: Condensed Matter*, **25**, Article ID: 295502.
- [38] Willett, R.D., Liles, O.L. and Michelson, C. (1967) Electronic Absorption Spectra of Monomeric Copper (II) Chloride Species and the Electron Spin Resonance Spectrum of the Square-Planar CuCl_{4-2} - Ion. *Inorganic Chemistry*, **6**, 1885-1889. <https://doi.org/10.1021/ic50056a028>
- [39] Choudalakis, G. and Gotsis, A.D. (2009) Permeability of Polymer/Clay Nanocomposites: A Review. *European Polymer Journal*, **45**, 967-984. <https://doi.org/10.1016/j.eurpolymj.2009.01.027>
- [40] Christians, J.A., Fung, R.C.M. and Kamat, P.V. (2013) An Inorganic Hole Conduc-

tor for Organo-Lead Halide Perovskite Solar Cells. Improved Hole Conductivity with Copper Iodide. *Journal of the American Chemical Society*, **136**, 758-764.
<https://doi.org/10.1021/ja411014k>

- [41] Stejskal, J. and Gilbert, R.G. (2002) Polyaniline. Preparation of a Conducting Polymer (IUPAC Technical Report). *Pure and Applied Chemistry*, **74**, 857-867.
<https://doi.org/10.1351/pac200274050857>
- [42] Im, J.-H., Jang, I.H., Pellet, N., Grätzel, M. and Park, N.-G. (2014) Growth of $\text{CH}_3\text{NH}_3\text{PbI}_3$ Cuboids with Controlled Size for High-Efficiency Perovskite Solar Cells. *Nature Nanotechnology*, **9**, 927-932. <https://doi.org/10.1038/nnano.2014.181>
- [43] Bruker (2008) Topas, Version 4.1. Bruker AXS Inc., Madison.
- [44] Kimishima, Y. (1980) The Magnetic Behaviors of Quasi-Two Dimensional Antiferromagnet $(\text{CH}_3\text{NH}_3)_2\text{CuBr}_4$. *Journal of the Physical Society of Japan*, **49**, 62-66.
<https://doi.org/10.1143/JPSJ.49.62>
- [45] Dualeh, A., Tétreault, N., Moehl, T., Gao, P., Nazeeruddin, M.K. and Grätzel, M. (2014) Effect of Annealing Temperature on Film Morphology of Organic-Inorganic Hybrid Pervoskite Solid-State Solar Cells. *Advanced Functional Materials*, **24**, 3250-3258. <https://doi.org/10.1002/adfm.201304022>